Desalination and Water Treatment
www.deswater.com

doi: 10.5004/dwt.2019.23996

152 (2019) 338–350
June

Adsorption of toxic heavy metals onto organofunctionalized acid activated exfoliated bentonite clay for achieving wastewater treatment goals

Farnaz Fazlali[a], Ali Reza Mahjoub[a,*], Hassan Aghayan[b]

[a]*Department of Chemistry, Tarbiat Modares University, P.O. Box. 14155-4383 Tehran, Iran, Tel. +98 21 82883442; emails: mahjouba@modares.ac.ir (A.R. Mahjoub), farnaz.fazlali@modares.ac.ir (F. Fazlali)*
[b]*Material and Nuclear Fuel Research School, Nuclear Science and Technology Research Institute (NSTRI), P.O. Box. 11365-8486, Tehran, Iran, email: hasanaghayan@yahoo.com*

Received 19 October 2018; Accepted 19 February 2019

ABSTRACT

This research focused on developing an effective method of using thiol modification acid activated exfoliated bentonite clay with good performance to remove four key toxic ions (As^{3+}, Hg^{2+}, Cd^{2+}, and Pb^{2+}) from water. A novel, low-cost, and locally available sorbent with high adsorption capacity comprising exfoliated organofunctionalized bentonite clay from Qazvin, Iran, was synthesized. To improve the sorption efficiency of acid activated bentonite (AB), clay was exfoliated (EAB) and then immobilized in toluene with addition of 3-mercaptopropyl trimethoxysilane (MPTMS) as a modifier (MEAB). The MEAB greatly increased removal of the four target ions. This study demonstrated that MEAB shows identical or even better sorption capacities compared with other conventional sorbents and that the binding capacity of heavy metal ions is about four times higher compared with unfunctionalized samples. The attachment of MPTMS to the exfoliated bentonite was confirmed by Fourier transform infrared spectroscopy (FTIR). Influential parameters including time, sorbent dosages, primary ions concentration, pH, and turbulence were investigated. Equilibrium facts were appraised by Langmuir and Freundlich isotherm models, while the toxic metal ions sorption reaction kinetics was explicated by Lagergren pseudo-first/second-order kinetic models. The results provided a mechanism of sorption including primarily ion complexation by a specific thiol group instead of unspecific cation exchange. As a consequence, this new functionalized exfoliated bentonite may be a good alternative to economical adsorbents for the elimination of toxic and hazardous heavy metals.

Keywords: Adsorption; Exfoliated bentonite; Thiol modification; Toxic metal

---

1. Introduction

Nowadays, water pollution is a very parlous and prevalent problem in our world [1], caused by hazardous and toxic heavy metal ions as a result of innumerable industrial actions, such as explosives manufacturing, metal chemical engineering, photographic materials, agriculture, ceramics, printing, and mining [2–4]. Due to the extreme effects of this problem on human's health as well as animal's health and aquatic life, many scientists and environmentalists have attracted deep attention for solving these serious problems [5]. These days, due to the industry's progress, we face a sharp rise in industrial wastewater containing a high amount of heavy metals such as Hg(II) [6], As(III) [7–9], Cd(II) [10,11], and Pb(II) [12,13], particularly in developing countries. These toxic heavy metal ions are of substantial importance inasmuch as they are not biodegradable and metabolized through the ambiance and have a tendency to accumulate in key organisms [14]. The health effects that toxic heavy metals can cause are as follows: skin corrosion, encephalopathy, gastrointestinal illness, hepatitis, kidney damage, diarrhea, reduced lung function [15–17], and finally, it can be

---

* Corresponding author.

claimed that these heavy metals cause irreparable effects on the main organs of the body, such as the heart, kidney, liver, and brain and may even cause death [18]. Because of the dire effects of these hazardous metals, it is essential to get rid of toxic ions from water before they log into the environment so that we can maintain stability and health in the ecosystem. There are many traditional methods to sequester toxic heavy metal ions from water, such as flotation or filtration [19], electrolytic recovery, chemical precipitation [20], carbon nanotubes sorbents [21], membrane processes [22], and ion exchange [23,24]. Each technique has its own advantages and limitations in use for many reasons, such as low efficiency, incomplete removal, high cost, requiring complicated instruments, and sometimes producing a large amount of waste that is too hard to remove. To overcome these drawbacks, one of the most useful, time efficient, and beneficial methods with large-scale applicability is sorption [25,26], because this method has many merits, such as flexibility, high treatment revenue, being cost-effective and eco-friendly, easy procedure, and we can also use naturally accessible sorbents in this effective method [27,28]. Using natural clays as sorbents plays a very important and helpful role in the environment by sorbing anions and cations [29]. In recent years, the usage of natural sorbents such as montmorillonite clay has attracted considerable attention because of their inapproachable properties such as low price, extensive specific area, vigorous adsorptive affinity, approachability, and simple usability, microporosity, layered structure, plasticity, and great cation interchange capacity [30–32]. Activated carbon is considered one of the most effective sorbents, but it is expensive, has a limitation in most factories and industries, and is hard to retrieve [33,34]. Therefore, the use of inexpensive supplies as sorbents for metal elimination from water has been the main focus. In this study, we selected generally obtainable sorbents, namely bentonite, which has a very low price [35,36], wonderful properties, and extensive use in industry [37]. Bentonite clay is the commonest phyllosilicate mineral composed of montmorillonite and 2:1 type with two silica tetrahedral sheets sandwiching an intermediate octahedral sheet [32]. Owing to the isomorphous substitution of Al^{3+}/$Si^{4+}$and Mg^{2+}/Al^{3+} in a crystal structure with a lower valence cation, we have a net negative charge in this clay [38,39]. One of the general problems with this clay is the relatively low surface area, so the external surface area of this clay can be significantly greater than before by exfoliation, which in turn improves the sorption proficiency and increases the catalyst's function [40]. Many recent studies have shown that selectivity and usefulness in the uptake of pollutant agents such as heavy metals is closely related to the physical and chemical features of the sorbents composition. Exfoliated bentonite clay is an effective sorbent, but some toxic ions are poorly adsorbed onto it. To resolve this moot point, chemical or physical alteration of the surface exfoliated bentonite clay by specified functional groups having several donor atoms such as sulfur, oxygen, phosphorus, and nitrogen is needed [41]. Functionalization of clay by thiol makes supplies that are selective and have a keen binding affinity for these heavy metal ions (As^{3+}, Hg^{2+}, Cd^{2+}, and Pb^{2+}), as a result of a soft Lewis acid/base reaction. Functionalized clay will prepare highly special sorption sites to increase the sorption capacity. Here, these metal ions are Lewis acids and functionalized groups such as phosphine, thiol, thiocyanate, and hydride are Lewis bases, and because of the strong gravity between acids and bases, we will have the covalent bonds forming, and finally, an increase in sorption is the benefit of this modification [42,43]. The thiol group tends to show a superior selectivity and strong connection for some heavy metal ions such as Zn^{2+}, Ag^{+}, Cd^{2+}, As^{3+}, Cu^{2+}, and Hg^{2+} [44]. The functionalization procedure which was carried out here follows the usual strategy for silica gel modification. This mechanism involves direct condensation interaction between the thiol group and the hydroxyl groups in the clay minerals [45]. In recent years, scientists have shown great interest in using thiol groups as a modifier of sorbents to increase the selectivity of removing heavy metal ions from water [18,41,43]. In Iran, the bentonite from Qazvin has been chosen as a capable nomination for removing wastewater disposal. If bentonite clay is exfoliated and the organosilanes are to be grafting on nano-layer external surfaces of exfoliated bentonite, they will show better sorption properties. The authors of this article are unaware of the existence of other articles that explain the functionalization of exfoliated bentonite by organosilanes. The main aim of this paper was to show that the exfoliation and functionalization of this cheap and green local bentonite with thiol groups provided by this most simple laboratory process can produce exceptional sorbents. This organization has numerous benefits: The procedure does not create another waste and all the samples involved can be reused and easily used on an industrial scale. A summary of the most important goals of this research is as follows: (1) to characterize the raw Iranian bentonite, exfoliated bentonite, and functionalized exfoliated bentonite samples using different analyses, such as transmission electron microscopy (TEM) and Fourier transformed infrared spectroscopy (FTIR); (2) to investigate the effectiveness of various parameters, such as interaction time, primary concentration of these toxic metal ions, pH solution, temperature on Cd^{2+}, Hg^{2+}, Pb^{2+}, and As^{3+} sorption using a batch technique.

2. Experimental setup

2.1. Materials and methods

All chemical materials used in this research were of analytical grade and used without extra purification. Double distilled water was used in all stages of the reaction. All laboratory glassware were held inside a 15% (v/v) HNO_3 solution for 24 h and at the end bathed by double distilled water. The bentonite clay (B) used in this study was extracted quite naturally from minerals in Qazvin, Iran. Materials used for the preparation of acid activated bentonite (AB) and exfoliated natural bentonite (EAB) were: hydrochloric acid (HCl), acetone, sodium fluoride (NaF), sodium hexametaphosphate $(NaPO_3)_6$, and distilled water.

Reagents used to immobilize thiol groups onto exfoliated bentonite (MEAB) included the following:

3-mercaptopropyl trimethoxysilane (MPTMS) ($HS–CH_2–CH_2–CH_2–Si–(OCH_3)_3$), dry toluene (99.8%), and acetone, which were supplied by Sigma-Aldrich (Italy) and Merck company (Darmstadt). Mercury, lead, arsenic, and cadmium polluted water solutions were organized via dissolving their salts (mercury nitrate monohydrate) Hg $(NO_3)_2·H_2O$, lead nitrate-Pb $(NO_3)_2$, arsenic trioxide-(As_2o_3), and cadmium nitrate ($Cd\ (NO_3)_2{\cdot}4H_2O$) into water (DI). All these salts were obtained from Merck company.

2.2. Synthesis of acid activated exfoliated bentonite

The natural bentonite was sieved, crushed, and ground through a 200 mesh size, then it was washed with distilled water numerous times to eliminate any impurities. It was then dispersed in deionized water. The mixture, which contained bentonite and distilled water, was stirred for 12 h and then kept without any movement for 2 d. After that, the resultant solution was centrifuged for three times and then was dried in a vacuum oven for hours. After this level, the remaining precipitation was washed with acid to remove silica and iron oxides. To do this procedure, 5 g of washed bentonite in the previous step was added to 100 mL of HCl solution (0.1 M), and was stirred for 8 h. The content was centrifuged and frequently washed with distilled water to wash off all the remaining acid and then was dried in oven at 60°C [46].

2.3. Steps in the synthesis of exfoliated bentonite

5 g acid activated bentonite (AB) was added to 100 mL water and the mixture was stirred for 1 h at room temperature, and then 0.2 g of NaF was added. Next the mixture was stirred at 90°C with 720 rpm. After 120 min, 0.025 g $(NaPO_3)_6$ was added to the mixture and was stirred at high speed. After dispersion for 40 min, the mixture was exposed to ultrasound for 60 min. In the next step, the mixture was placed at room temperature for 48 h without any movement, then the supernatant was centrifuged at the highest possible speed (1400 rpm), to extract a colloidal fraction because this colloidal fraction is the synthesized exfoliated bentonite that was used in all the tests [40].

2.4. Thiol functionalization of acid activated exfoliated bentonite

The modification procedure of grafting exfoliated bentonite using MPTMS was carried out through the following steps: 5 g of exfoliated bentonite was dispersed in 300 cm^3 of 2 mL MTMPS in dry toluene. The mixture was refluxed through nonstop stirring at 25°C for 48 h in Ar atmosphere to prevent the oxidation of the thiol groups. Next, the solid obtained from the previous step was washed repeatedly with pure and dry toluene to eliminate any non-bonded silane and then centrifuged for 30 min and dried for 1 d at 60°C under vacuum conditions. The functionalized process and immobilized (–SH) groups were comparable with that described by Walcarius [42]. The steps involved in the synthesis of this sorbent are shown in Fig. 1.

2.5. Tools for characterization

X-ray diffraction (XRD) analysis of the prepared samples was carried out by Philips X'Pert X-ray diffractometer, and Cu Kα radiation (wavelength, $\lambda = 1.5481$ Å) was used as the radiation source to affirm the crystalline building of the samples at ambient temperature. All of the synthesized samples were skimmed from 0° to 80° through a step range of 0.033° in 2θ.

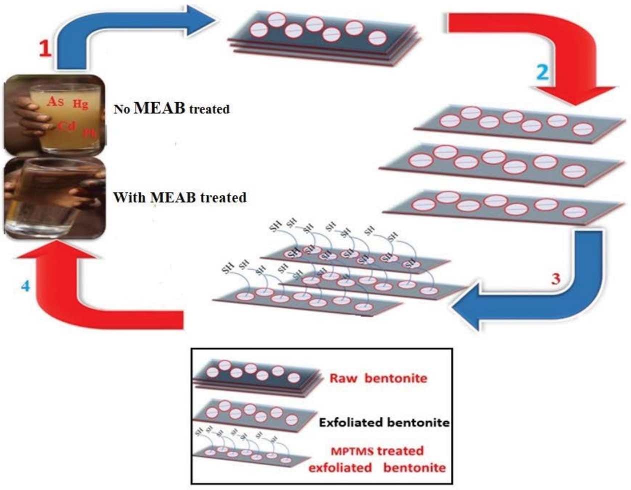

Fig. 1. Overall steps applied for preparing of MEAB.

The morphology and textural structures for all samples were assayed by scanning electron microscopy (Philips XL-300 instrument, Holland), and TEM (Philips CM 30 Holland). The existence of the thiol modification and other functional groups on acid activated exfoliated bentonite was attested by FTIR spectra (Shimadzu-8400S spectrometer, Japan). Heavy metal ion concentration of all samples at diverse times was analyzed using inductively coupled plasma atomic emission spectroscopy (ICP) (Varian vista-PRO device). The surface areas and the pore features of the natural sorbents were measured by Brunauer–Emmett–Teller (BET) technique and Barrett–Joyner–Halenda. pH adjustments were accomplished by a Metrohm model 713 (Herisau, Switzerland) pH-meter.

2.6. Heavy metal sorption examinations

For a better understanding of the sorption manner of the modifying sorbent, both methods including kinetics and isotherm sorptions were investigated [47]. For the first purpose of the study the kinetics of the sorption procedure on functionalized exfoliated bentonite, 10 mg of the synthesized sorbent was added per 20 mL of polluted water solutions with continuous mechanical stirring at room temperature. The standard solution was used to form dilute solutions of diverse working concentrations (100–500 mg/L). The pH of the solution was changed to values ranging from 2.0 to 8.0 by the dropwise addition of 0.1 M NaOH or 0.1 M HCl when required. At different intervals in time, the different concentrations of the heavy metals were determined, and eventually, investigated by ICP analysis. The effects of the experimental factors on the sorption capacity of functionalized exfoliated bentonite in the test were investigated. The following equation was used to achieve the sorption capacity of heavy metal ions.

$$\text{Sorption capacity}\left(q_t\right)\left(\text{mg/g}\right) = \frac{C_0 - C_t}{M} \times V \tag{1}$$

where M indicates the mass of our natural sorbent (g), V is the whole volume of the water solution (mL), C_0 (mg L^{-1}) and

C_t (mg L^{-1}) are the concentrations of heavy metal ions (ppm) in the watery phase initially and at time *t*, respectively.

For the second purpose of the study, the sorption isotherms were achieved by adding the functionalized exfoliated bentonite to polluted water solutions with diverse primary heavy metal ion concentrations extending from 10 to 1,000 ppm. This test was accomplished at 25°C for 12 h on a shaker instrument working at 150 rpm. After 12 h, the concentration of the toxic heavy metal ions for the separated water solution was evaluated by ICP, and the equilibrium sorption of every ion was then analyzed by Eq. (2), where C_e is substituted by the equilibrium ion concentration.

$$\text{Adsorption capacity}\left(q_e\right)\left(\text{mg/g}\right)=\frac{C_0-C_e}{m}\times V \tag{2}$$

It was also calculated using Eq. (3) for the percentage of removal efficiency:

$$\text{Removal efficiency}\left(\%\right)=\frac{C_0-C_e}{C_0}\times 100 \tag{3}$$

3. Results and discussion

3.1. Structure, feature, and function of the MPTMS treated exfoliated bentonite

3.1.1. FTIR analysis

The FTIR spectra of B, AB, EAB pure MPTMS, and MEAB are used to analyze the properties of sorbents such as construction and interactions, as shown in Fig. 2. Infrared spectroscopy is very sensitive to functionalization of this natural clay mineral construction by MPTMS modifier. The FTIR spectra for the natural clay showed deep band taking place near 3,437 cm^{-1} owing to O–H stretching vibration of the silanol (Si–OH) and (Al–OH) groups from the solid surface and the spectral peak at 1,628 cm^{-1} attributed to the angular deformation of H–OH bond of free water molecules, which is restrained in environment. According to the usual montmorillonite pattern the strong band taking place near 3,628 cm^{-1} is attributed to the stretching vibration of structural hydroxyl groups such as the Mg–OH, Al–OH [25]. In all FTIR analyses, the power of the stretching vibration for hydroxyl groups at 3,628 cm^{-1} decreases after the acid behavior because of the elimination of octahedral [48]. The other broad peaks at 1,028 cm^{-1} are related to Si–O stretching vibrations of a Si–O–Si tetrahedral sheet. The sharp band at 788 cm^{-1} represents the existence of quartz in Iranian bentonite clay. The peak situation at 920 cm^{-1} is attributed to the stretching vibration of Al–O–(OH)–Al [49]. As expected, the exfoliated treatment does not show significant changes between the natural bentonite and the exfoliated bentonite. Moreover, to further approve the existence of thiol on exfoliated bentonite, an FTIR was used. Pure MPTMS was used as a reference for better comparison. In the pure MPTMS FTIR analysis, the weak band at 2,555 cm^{-1} displayed the existence of SH group [42,50]. The sorption peaks detected in 2,820–3,000 cm^{-1} are related to the aliphatic CH stretching vibrations [51]. In the MPTMS treated exfoliated bentonite, FTIR data showed the existence of adsorption at 2,555 cm^{-1}. Caused by the aboriginal character of the thiol group sorption and the little SH level introduced onto exfoliated bentonite, the 2,555 cm^{-1} bands befitted even feebler after the functionalization of the exfoliated bentonite surface. The peaks at 2,944 and 2,845 cm^{-1} both indicated the asymmetric stretching vibration of CH_2 and CH_3. The adsorption peak at 1,445 cm^{-1} is also related to the bending vibrations CH_2 and CH_3. In the low energy area, the sorption peak at 1,038 cm^{-1} was owing to the Si–O–Si and Si–O stretching. On the other hand, the blue shift of these peaks for thiol groups treated exfoliated bentonite samples in comparison with pure vibration peaks affirmed the existence of the conjunction $-CH_2-CH_2-CH_2-SH$ molecules. Consequently, FTIR information confirmed the effective incorporation of SH (thiol) onto exfoliated bentonite [44].

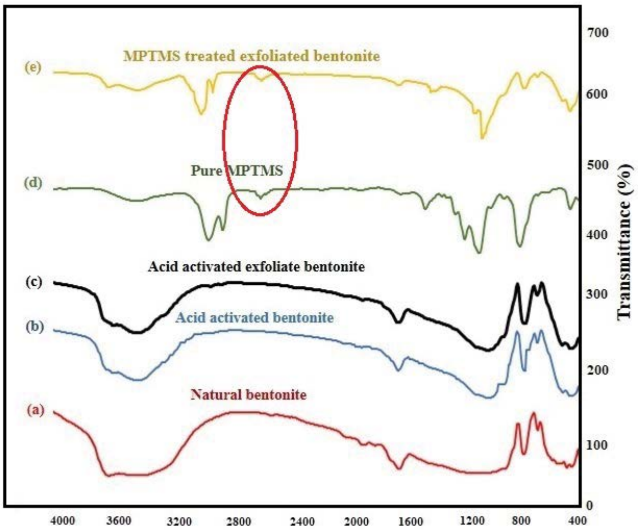

Fig. 2. FTIR spectra of raw bentonite clay (B) (a), acid activated bentonite clay (AB) (b), acid activated exfoliated bentonite clay (EAB) (c), pure MPTMS (d), MPTMS treated exfoliated bentonite (MEAB) (e).

3.1.2. SEM@EDX observations

The surface morphologies of B, EAB, and MEAB were studied using SEM. The picture of pristine and raw bentonite (Fig. 3(a)) obviously reveals the rough and uneven surfaces with numerous crumples. The surface of pure bentonite clay has plenty of leaf-like sheets that come from the bentonite fundamental morphology. As for the morphology of exfoliated bentonite (Fig. 3(b)), one can see that both the crumpled structure and compact surfaces are lower, and the sheets of clay are in some measure exfoliated and reorganized. Unsurprisingly, the thiol group functionalization (Fig. 3(c)) does not lead to noticeable surface alterations, as functionalization is a kind of surface treatment equipment, as demonstrated earlier, but one can see that it is thin and somewhat crumpled with little agglomerations.

We also used EDX analysis before and after EAB to further verify the presence of thiol group in the sample (Fig. 3(d)).

ICP atomic emission spectroscopy of S showed that 1 g of thiol functionalized acid activated exfoliated bentonite included (0.51 ± 0.01 g of MPTMS or 3.4 mmol of S).

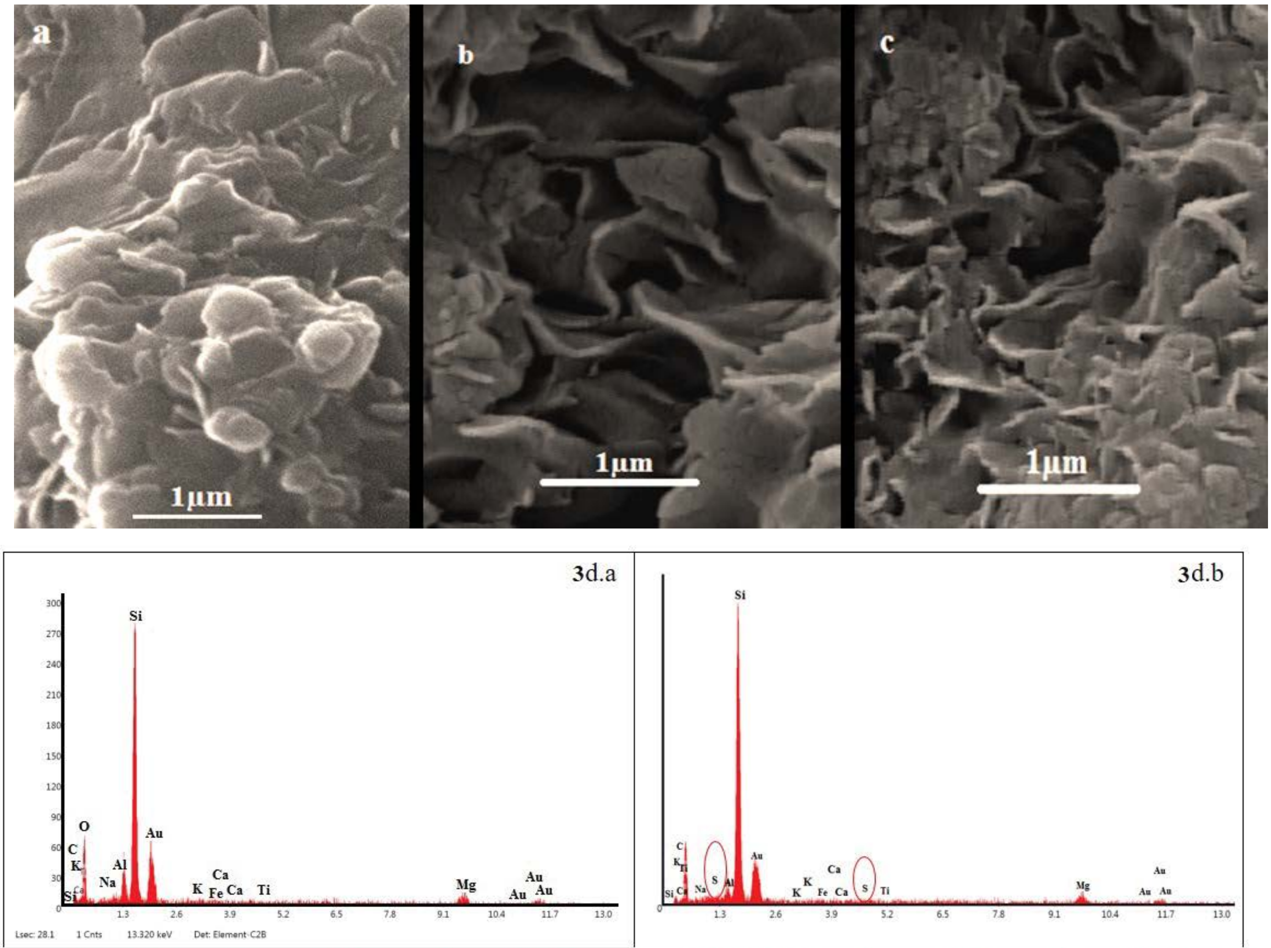

ELEMENT	Wt%	At%
O K	35.08	43.96
Al K	6.19	4.53
Si K	27.01	19.03
Na K	5.32	4.56
Ca K	0.35	0.17
Mg K	2.99	2.79
Ti K	0.27	0.11
S K	0	0
K K	0.56	0.28

ELEMENT	Wt%	At%
O K	35.68	44.4
Al K	4.16	3.07
Si K	30.67	21.74
Na K	6.98	6.04
Ca K	0.19	0.09
Mg K	2.81	2.01
Ti K	0.29	0.12
S K	1.63	1.39
K K	0.22	0.11

Fig. 3. SEM images of the raw Iranian bentonite clay (B) (a), exfoliated bentonite (EAB) (b), MPTMS treated exfoliated bentonite (MEAB) (c).EDX images EAB (3d,a) and MEAB (3d,b).

3.1.3. TEM analysis

The morphology of exfoliated bentonite was considered by TEM analysis. The layered construction of pristine bentonite had been naked into extremely thin layers (Fig. 4), which might supply a sufficient surface region to not only adsorb contaminants but also to be in close interaction with a modifier.

3.1.4. XRD patterns

The XRD patterns of B (a), AB (b), EAB (c), and MEAB (d) are shown in Fig. 5. XRD is a nondestructive and systematic method, which exposes evidence about the crystallographic construction of the sample under investigation. The method is extensively used in the identification of clays. The XRD pattern of pristine bentonite indicated the d001 reflection at 2θ = 5.6, offering the c-axis dimension of 1.46 nm, which is specific to montmorillonite as expected [52]. For exfoliated bentonite, the typical peak of bentonite at 2θ is wide, extensive, and weak, which proposed the fact that the layers of this clay were delaminated by the exfoliation process [40]. For MEAB, as expected, XRD data show that the thiol behavior does not alter the exfoliated bentonite crystalline structure, as exposed through the similar specific diffraction band situations in both the thiol treated exfoliated bentonite and exfoliated bentonite.

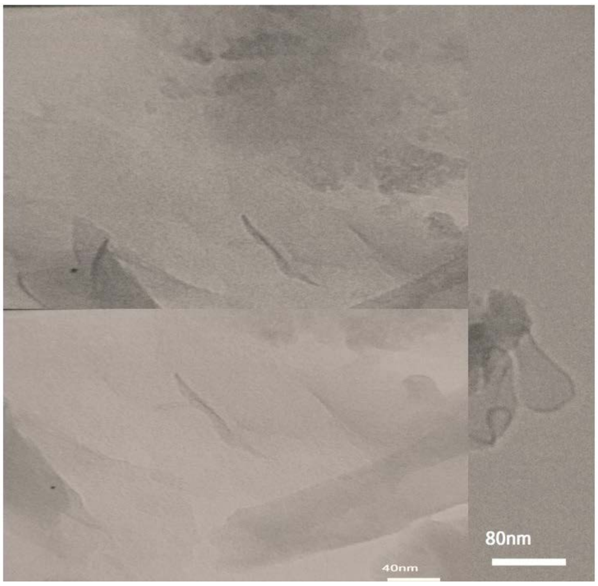

Fig. 4. TEM images of MEAB.

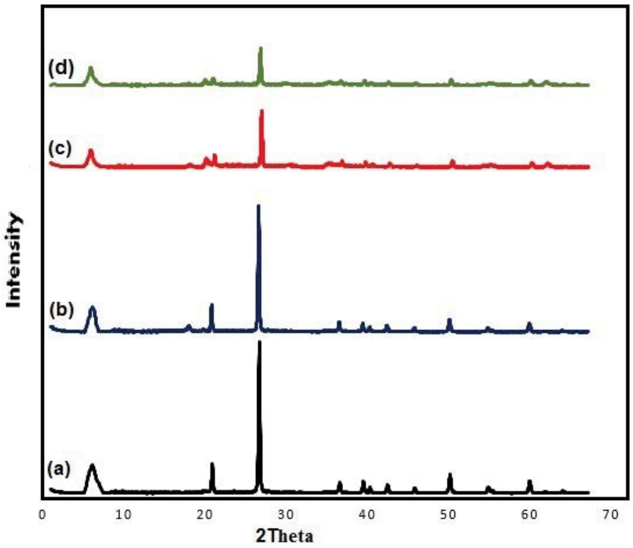

Fig. 5. High-angle XRD patterns of pristine bentonite (B) (a), acid activated bentonite (AB) (b), acid activated exfoliated bentonite (EAB) (c), MPTMS treated exfoliated bentonite (MEAB) (d).

Table 1
Effect of the modification process on the surface area (BET), average pore size distribution and pore volume of all samples

Samples	BET surface area (m^2 g^{-1})	Average pore diameters (nm)	Pore volume (cm^3 g^{-1})
B	69.6	3.7	0.081
AB	113	3.6	0.088
EAB	222	3.5	0.091
MEAB	60.0	12.4	0.032

3.1.5. BET analysis

The specific surface areas of B, AB, EAB, and MEAB were determined to be 69.6, 113, 222, and 60.0 m^{2}g^{-1}, respectively. Substantial changes in nitrogen sorption–desorption were detected upon raw bentonite, acid behavior, exfoliated bentonite, and finally grafting. Acid activation increased the specific surface area, and also the pore volumes (S_{BET}: 69–113 m^2 g^{-1}), after acid behavior, deeply increased after the exfoliation process (S_{BET}: 222 m^2 g^{-1}) and powerfully decreased after being treated with MPTMS (S_{BET}: 11 m^2 g^{-1}; Table 1). Pores may have been approximately engaged or blocked through the modifying agent. The amplification of the ordinary pore diameter was owing to the decrease of microporous contribution and led to a greater value of pore size. Comparable comments were reported by Walcarius [53], that amorphous silica gels were modified by amine and thiol groups.

3.2. Kinetic and equilibrium studies

It is well settled that a number of factors such as pH, the concentration of a heavy metal ion, time, the amount of sorbent, turbulence, and solution temperature are highly effective on the useful sorption of a toxic metal ion [53]. Optimization of As(III), Pb(II), Hg(II), and Cd(II) sorption represented that the highest elimination was achieved in the solution embracing 30 ppm metal ions with 30 mg of synthesized sorbent at 25°C, pH = 8, and 30 min of contact time with 200 rpm turbulence. The results of different factors on the sorption percentage of As(III), Pb(II), Hg(II), and Cd(II) have been reported in detail as follows:

3.2.1. Effect of solution pH on the sorption of heavy metal ions

The effect of the pH on the removal of As(III), Pb(II), Hg(II), and Cd(II) ions was studied in numerous pH ranges (2–8) [54]. The pH variety was selected as 2–8 for the purpose of eluding precipitation of cations in the hydroxide or chloride form. Moreover, by increasing the amount of pH in this process, the probability of hydroxide formation of the metal ions is minimized due to chemical precipitation. The pH of a solution is a key factor affecting the elimination of toxic heavy metal ions from aqueous solutions. The dependency of heavy metal sorption on pH is due to two reasons. The first reason is about the heavy metal chemistry in the mixture and the second reason is related to the ionization situation of the functional groups of the sorbent, which impress the accessibility of binding positions. 0.03 g of the prepared sorbent was dissolved in a 20 mL solution of 30 mg L^{-1} of metal ions at diverse pH values (2, 3, 4, 5, 6, 7, and 8). The pH adjustment of all solutions was achieved by HCl (0.1 M) and NaOH (0.1 M). All the samples were stirred for 240 min at 200 rpm, and then centrifuged for 4 min to separate the sorbent. The results are reported in Fig. 6.

As seen in the figure, the metal ions removal at low pH values is insignificant. Nevertheless, removal effectiveness increases slowly with increasing pH. To better emphasize on the subject of pH effect, the pH$_{pzc}$ analysis was applied. As defined in the figure, higher pH leads to greater heavy metal uptake. Acid conditions are not appropriate for fierce competition between protons, and different types of heavy

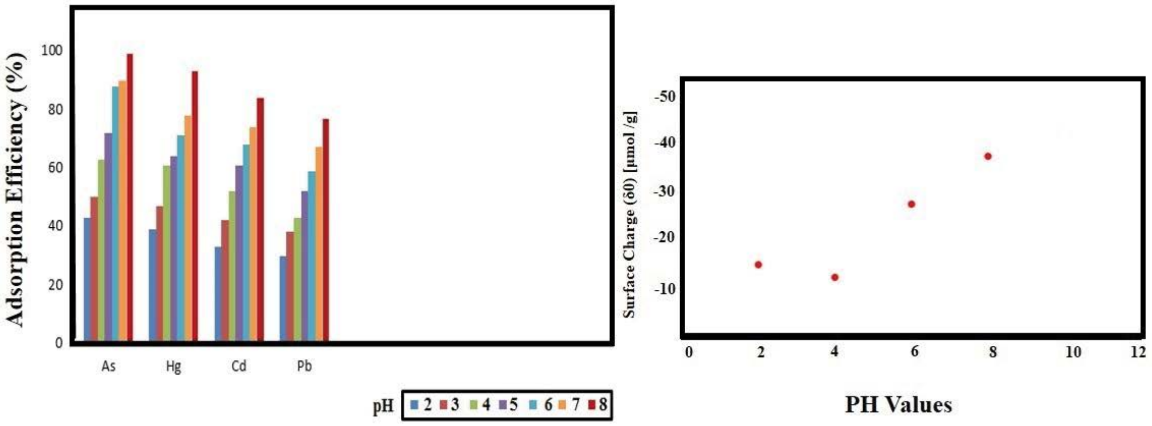

Fig. 6. Effect of solution pH importance on the sorption of heavy metal ions.

metals can consequently clarify the medium sorption in the optimum amount of acid. The maximum uptake rate was noted at the pH of 8. This could be imputed to the tendency of free lone pair electrons on thiol groups and oxygen atoms without protons, which are appropriate for coordination by the heavy metal ions.

3.2.2. Effect of sorbent dosage on the sorption of heavy metal ions

We deliberated the affinity of the sorption of metal ions on the measure of functionalized exfoliated clay at pH 8 and room temperature via variable sorbent extents from 0.01 to 0.06 g in contact with the 20 mL solution of the mixture of 10 mg L^{-1} of each of the toxic metal ions. Next, the mixture was stirred for 240 min with a shaker, and after centrifuging, the supernatant was investigated. The consequences are shown in Fig. 7. Seemingly, from the investigational facts, the percentage of the elimination of the metal ions improved inchmeal by increasing the measure of the modified sorbent, which is due to the greater availability of the sorbent. This may be associated with the growth of active sorption sites for the deletion of toxic metal ions. Finally, by increasing the sorbent amount, the sorption was highest with 0.03 g of the sorbent for all metal ions, and the highest percentage elimination was about 99% for arsenic ions.

3.2.3. Effect of primary metal ion concentration on the sorption procedure

The primary toxic metal ion concentration is able to influence the rate of sorption procedure, which makes it a key factor to be considered for well-organized sorption. To achieve a clear vision about the mechanism of heavy metal sorption procedure and the capacity of the sorbent, experimental examinations were considered at diverse concentrations (5–60 ppm). As can be seen clearly in Fig. 8, the elimination percentage of toxic ions improved with the increase of metal ions up to 30. Extra increase in the primary concentration of toxic ions was escorted via a reduction in the elimination percentage. This process can be due to the saturation of the functional groups in active sites of the sorbent with the toxic ions at greater concentrations.

3.2.4. Effect of interaction time and turbulence speed on the sorption procedure

Stirring time is a factor that plays a key part in the sorption procedure of toxic ions onto the exfoliated bentonite

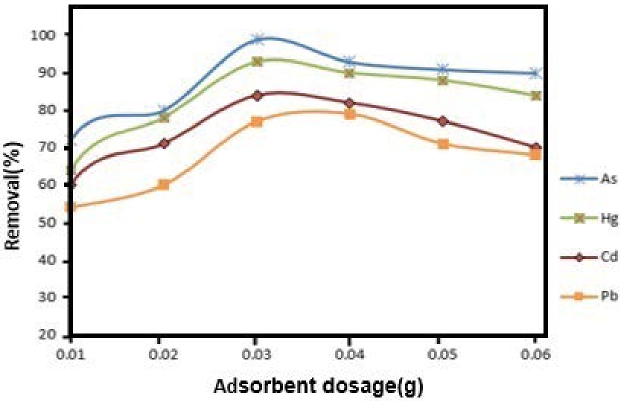

Fig. 7. Effect of sorbent dosage on the sorption of heavy metal ions.

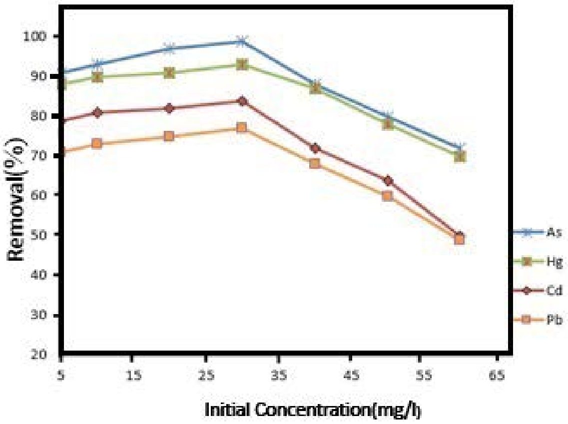

Fig. 8. Effect of primary metal ion concentration on the sorption procedure.

functional groups. These approaches are important for identification of the feasible speed of binding and elimination methods of the tested toxic ions through the newly functionalized sorbents and earning the optimal time for complete elimination of toxic metal ions. This factor has a noteworthy effect on saving money, time, and energy in the item of huge scale procedure. For this purpose, the kinetic tests were performed by mixing 30 mg of newly functionalized sorbents with 20 mL of toxic ions solution (C_0 = 30 mg L^{-1}). As can be seen in Fig. 9(a), the sorption process of sorbate was completed rapidly in the first 15 min. This primary speedy uptake of the target ions alluded to the availability of a lot of accessible active functional sites. Removal amount of these toxic ions was established to be balanced to the stirring time up to the equilibrium reached, after which it is free of time for the reason that the level of sorption and desorption will be equal at equilibrium.

The effect of turbulence speed was also considered at room temperature (stirring time of 15 min, 30 mg sorbent, 20 mL solution 30 mg L^{-1}, pH = 8). As shown in Fig. 9(b), it was clearly apperceived that via accelerating the turbulence rapidity from 100 to 400 rpm, the highest removal percentage of target ions were achieved up to 200 rpm. Therefore, at a turbulence rapidity of 200 rpm, the highest sorption was achieved for toxic metal ions.

3.3. Kinetic modeling

It is known that the acceleration of sorption is extremely essential in the design and estimate of synthesized sorbents in eliminating As(III), Pb(II), Hg(II), and Cd(II) from the wastewater solution. The kinetics for sorption of As(III), Pb(II), Hg(II), and Cd(II) onto organofunctionalized exfoliated bentonite was tested, and the results are reported in Table 2. With the aim of understanding entirely the sorption kinetics of each toxic metal ion, an organized time study was conducted [55]. In the study, exfoliated bentonite before and after MPTMS behavior was 30 ppm water solutions of As^{3+}, Cd^{2+}, Hg^{2+}, and Pb^{2+} for diverse sorption times: 5, 15, 30, 45, 60, 120, and 240 min. The ion sorption ranks at diverse time intermissions were then plotted contrary to sorption time, the consequences of which are shown in Fig. 10. It may be understood that exfoliated bentonite by MPTMS behavior confirmation improved toxic metal ion sorption being the highest for $As^{3+} >> Hg^{2+} > Cd^{2+}$ followed by Pb^{2+} as compared with the exfoliated bentonite without MPTMS behavior. This figure showed that the highest uptake rate occurred in the first 15 min for all toxic heavy metal ion solutions because of extraordinary affinity among the toxic ions, the organofunctionalized surface of exfoliated bentonites, and also a large number of accessible active sites. The accessible active sites of the synthesized organofunctionalized exfoliated bentonite for chelating of toxic ions. Succeeding, the equilibriums ensued at 30 min for all samples by the piecemeal reduction of these accessible active sites and the further growing of repulsive forces among cations previously adsorbed with the free positive ions in the solution. Two well-known kinetic models were used to consider the sorption mechanism. The kinetic mechanism of the organofunctionalized exfoliated bentonite was valued using pseudo-first-order and pseudo-second-order, which rein the sorption procedure.

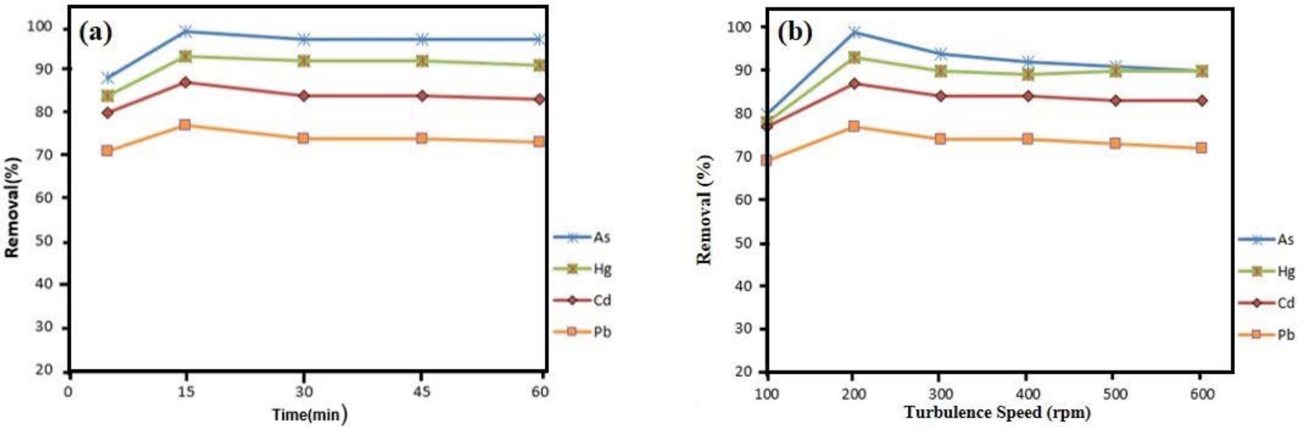

Fig. 9. Effect of interaction time (a) and turbulence speed (b) on the sorption procedure.

Table 2
Results based on the pseudo-first-order and pseudo-second-order kinetic models.

Metal ion	Pseudo-first-order			R^2	Pseudo-second-order		R^2
	q_{e1} (mg g^{-1})	k_1 (min^{-1})	$q_{e,Exp}$ (mg g^{-1})		k_2 (g mg^{-1} min^{-1})	q_{e2} (mg g^{-1})	
As^{3+}	3.2	0.01	42	0.953	9.2×10^{-4}	42.19	0.9868
Hg^{2+}	1.3	0.015	28	0.933	1.35×10^{-3}	28.08	1
Cd^{2+}	1.4	0.023	24	0.986	1.5×10^{-3}	25.77	0.9925
Pb^{2+}	1. 5	0.056	19	0.9831	2.3×10^{-3}	19.56	0.9973

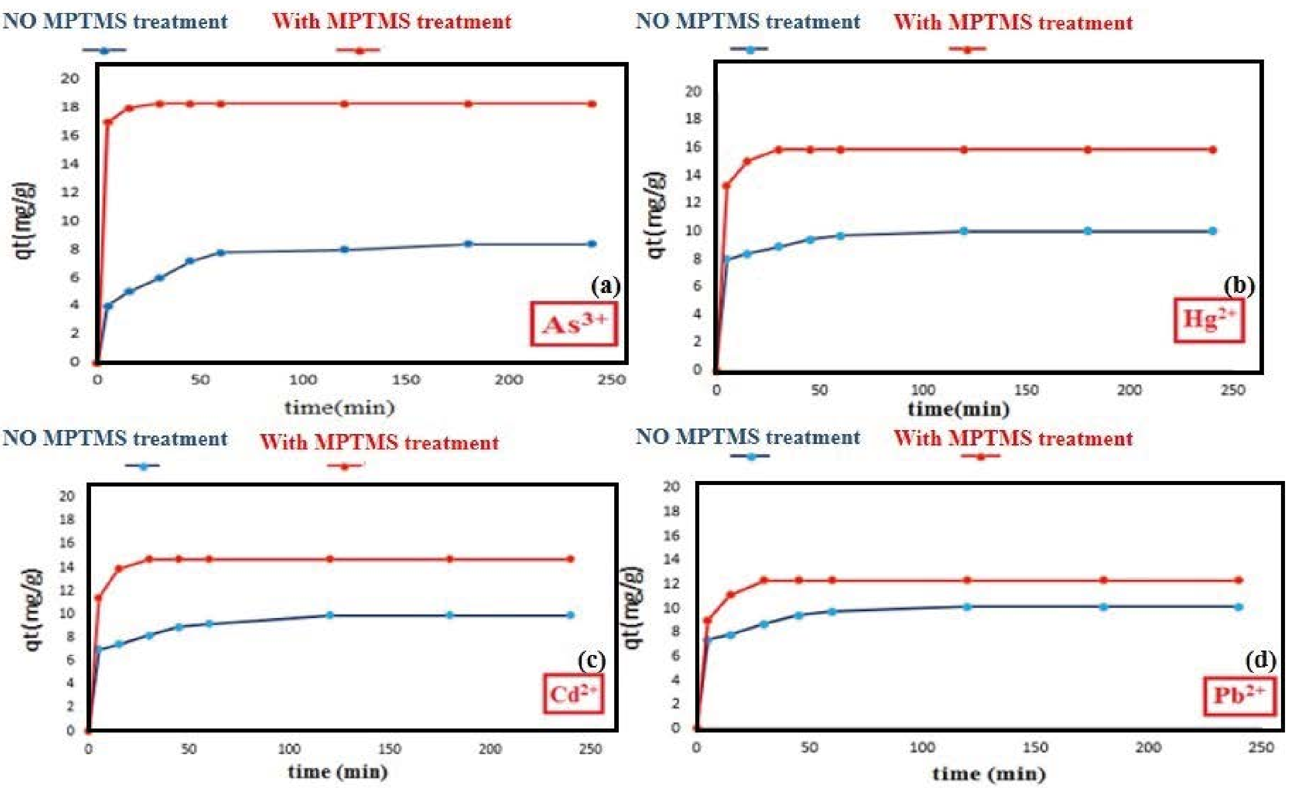

Fig. 10. Sorption kinetics consequences for exfoliated bentonite before and after MPTMS behavior exposed to (a) As^{3+}, (b) Hg^{2+}, (c) Cd^{2+}, and (d) Pb^{2+} water solutions.

3.3.1. Pseudo-first-order kinetics

The pseudo-first-order kinetics sorption pattern was recommended by Lagergren [56] for the sorption and can be evinced in two models, integrated and linear pattern.

The linear pattern of the pseudo-first-order equation can be displayed by Eq. (4), as follows:

$$\log\left(q_e - q_t\right) = \log q_e - \frac{k_1 t}{2.303} \tag{4}$$

where k_1 (L min^{-1}) is the pseudo-first-order rate constant of sorption, q_e and q_t are related to the amount of adsorbed toxic ions (mg g^{-1}) at equilibrium and t time (min), respectively.

Fig. 11(a) illustrates that the quantity of k_1 is assigned from the graphs of log ($q_e - q_t$) in competition with t for As(III), Pb(II), Hg(II), and Cd(II) ions. In this case, the amounts for R^2 are comparatively slight and the computed amounts which were achieved from the linear graphs do not coincide through the experimental q_e amounts.

3.3.2. Pseudo-second-order kinetics

This kinetic pattern has been extensively used for a large amount of toxic heavy metal ions–sorbent organizations. The pseudo-second-order kinetics pattern is:

$$\frac{t}{q_t} = \frac{1}{k_2 q_e^2} + \frac{1}{q_e} \times t \tag{5}$$

where k_2 (g mg^{-1} min^{-1}) is the pseudo-second-order rate constant of sorption. The activation energy can be assigned by the pseudo-second-order rate constants of the sorption procedure. In Fig. 11(b), the linear graph of t/q_t in competition with t is displayed. The acquired R^2 amounts are approximately near 1 for all toxic metal ions. The pseudo-second-order pattern is grounded on the obligation that the speed restrictive step can be chemisorption, which contains valence forces through electron interchange among the sorbent and the sorbate.

By likening the information of Fig. 11 and Table 2, the pseudo-second-order pattern was found to characterize the sorption procedure more successfully than the pseudo-first-order pattern. In addition, the results illustrated that As^{3+} has the fastest primary sorption rate among all toxic ions. Based on the obtained data, it is evident that the introduction of MPTMS (thiol group) onto exfoliated bentonite has significantly heightened the elimination rate of all four target toxic heavy metal ions with As^{3+} being the greatest effective toxic ion to be eliminated. These consequences are dependable through the extraordinary reactivity of As^{3+} toward the thiol (–SH) group along with the Pearson soft acid and base assumption.

3.4. Sorption modeling

The penchant of the sorbent for the sorbate may be defined via the isotherm equation, which is essential for the explanation of the sorption equilibrium. It can be understood

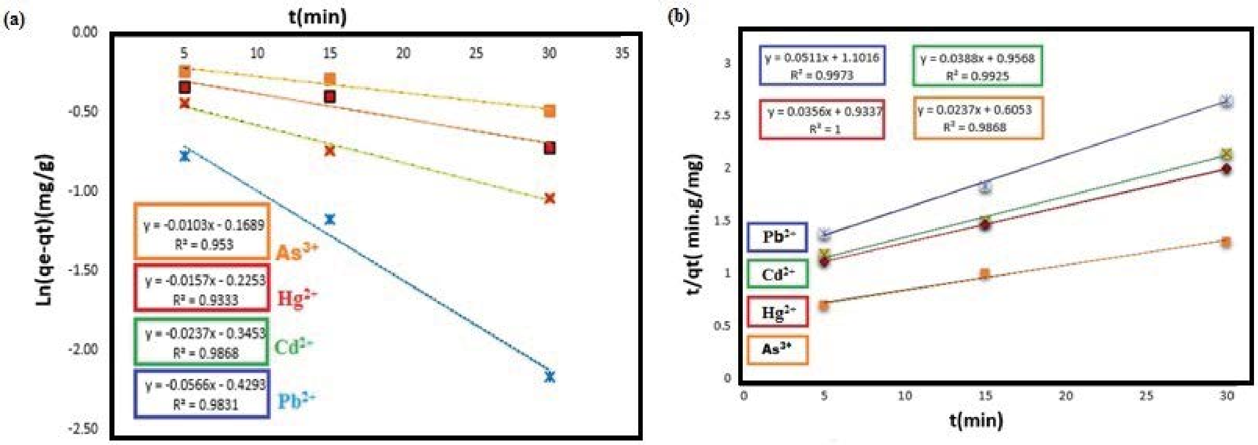

Fig. 11. Pseudo-first-order model fitting plots for As^{3+}, Hg^{2+}, Cd^{2+}, and Pb^{2+} sorption kinetics information (a), pseudo-second-order model fitting plots for As^{3+}, Hg^{2+}, Cd^{2+}, and Pb^{2+} sorption kinetics information (b).

from the sorption modeling circumstances that the sorbate ions are dispersed between the liquid and solid phases. It is imperative to acquire an accurate equilibrium connection between the concentrations of toxic ions and solid and liquid phases, for a better clarification of the sorbent proficiency. In this research, it was obligatory to study the acquired equilibrium information for elimination of As(III), Pb(II), Hg(II), and Cd(II) toxic ions using isotherm models, and a number of sorption factors were assigned from Langmuir and Freundlich isotherm models, which are extensively used sorption isotherms.

3.4.1. Langmuir isotherm

The Langmuir model has been extensively used to improve toxic ions sorption. The main objective of the Langmuir theory is that a monolayer sorption on a homogeneous surface is deprived of any interaction among adsorbed

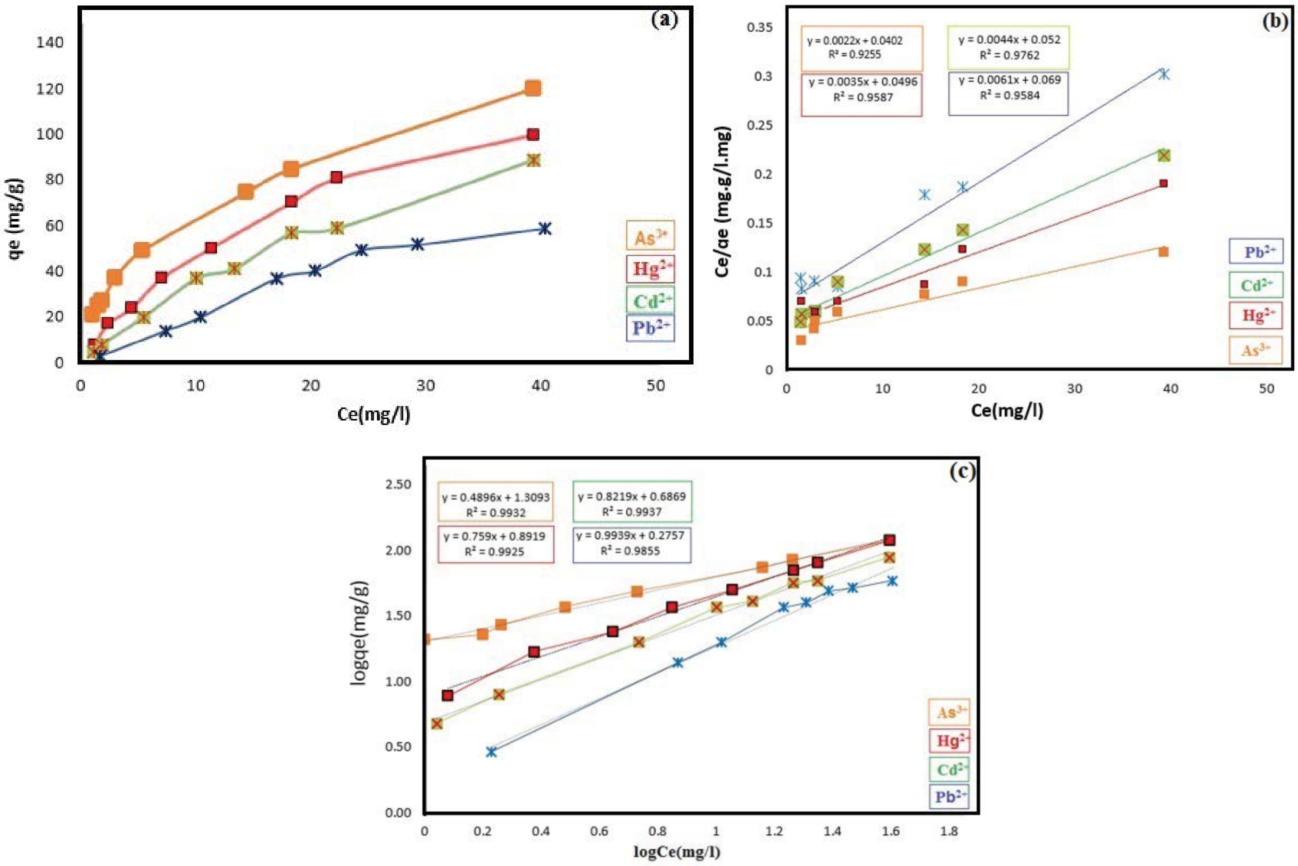

Fig. 12. Sorption isotherm of MEAB (a), linear Langmuir plot (b) linear Freundlich plot (c).

ions. Langmuir isotherm is dependent on either physical and chemical interaction or both individually which take place among the sorbate and the accessible available sites on the sorbent surface. This model also appears in the form of an equation:

$$\frac{C_e}{q_e} = \frac{1}{bq_m} + \frac{C_e}{q_m} \tag{6}$$

where q_e is the adsorbed quantity of metal ions (mg g^{-1}) at equilibrium, q_m is the utmost sorption capacity connecting to the whole monolayer coverage (mg g^{-1}), b (L mg^{-1}) is a constant corresponding to the energy of sorption, and C_e is the concentration of metal ions at equilibrium (mg L^{-1}). Fig. 12(b) clarifies the applicability of the Langmuir isotherm modeling for the present research through a linear plot C_e/q_e against C_e of the Langmuir isotherm modeling. The q_m quantities for As(III), Pb(II), Hg(II), and Cd(II) toxic ions were assigned from the slope/intercept of the reported linear graph. The consequences are obtainable in Table 3. The sorption capacities by MEAB and other sorbents are indicated in Table 4.

3.4.2. Freundlich isotherm

The Freundlich isotherm modeling is a tentative equation which assumes a multilayer sorption on a heterogeneous surface. This isotherm modeling states that the ratio of the quantity of toxic ions adsorbed onto a specified quantity of the sorbent to the concentration of the toxic ions in the solution is not permanent at diverse concentrations. The Freundlich sorption modeling, which is a connotation of surface heterogeneity for a sorbent, is expressed in the following equation:

$$q_e = \log k_f + \frac{1}{n}\log C_e \tag{7}$$

where k_f (L mg^{-1}) is Freundlich constants linked to the sorption intensity and sorption capacity, and $1/n$ (dimensionless) denotes the heterogeneity parameter. As shown in Fig. 12(c), the amounts of $1/n$ and k_f for all toxic metal ions were assigned from the slope and the intercept of the linear graphs which are accessible in Table 3.

Based on Table 3, it is obvious that, for all four toxic metal ions, samples fit the Freundlich model better than Langmuir model through comparing the R^2 valuation of both models.

Subsequently, the introduction of MPTMS (thiol group) and, the sorption performance of MPTMS treated exfoliated bentonite make the Freundlich model superior to the Langmuir model. As mentioned above, the Freundlich model assumes the heterogeneous interaction amid sorbent/sorbate and foretells non-monolayer cover. It is well assumed to that a multi-layer cover is attained in the thiol group treated exfoliated bentonite. The heterogeneous sorption in MPTMS (thiol group) treated exfoliated bentonite accedes by their surface properties.

Table 3
Langmuir and Freundlich factors for sorption of As^{3+}, Cd^{2+}, Hg^{2+}, and Pb^{2+} by MEAB

Metal ion	Langmuir			Freundlich		
	Q_m (mg g^{-1})	b (L mg^{-1})	R^2	k_f	n	R^2
As^{3+}	454.54	0.054	0.9255	20.4	2	0.9932
Hg^{2+}	285.71	0.07	0.9587	7.8	1.3	0.9925
Cd^{2+}	227.27	0.084	0.9762	4.9	1.2	0.9937
Pb^{2+}	163.93	0.088	0.9584	1.9	1	0.9855

3.5. Desorption and regeneration experiments

One of the most important factors in synthesized sorbents is to use them several times in the sorption process without having a perceptible change in the sorption capacity, which is a key issue in designing capable and cut-rate organization for treatment of contaminated water solutions [57]. The ICP analysis is utilized for investigation of steadiness of synthesized sorbents. The examination of the reusability of the sorbent revealed that the sorption–desorption cycle

Table 4
Comparison of sorption capacities (mg g^{-1}) for target toxic metal ions by numerous sorbents

Sorbent	As^{3+} (mg g^{-1})	Hg^{2+} (mg g^{-1})	Cd^{2+} (mg g^{-1})	Pb^{2+} (mg g^{-1})	References
Thiol- and amine bi functionalized mesoporous silica	14.4	–	–	–	[8]
Thiol-functionalized aluminum oxide hydroxide nanowhiskers	–	114	68	125	[41]
Thiol-functionalized magnetic sawdust	–	–	3.80	12.5	[43]
Nano-alumina modified with 2,4-dinitrophenylhydrazine	–	–	83.3	100	[57]
(NH_2 + SH) modified silica gel	2.7	–	–	–	[58]
CGMA-MAn-IDAc/Fe_3O_4–NH_2	–	–	48.53	53.33	[59]
Organofunctionalized exfoliated Iranian bentonite clay	454.54	285.71	227.27	163.93	This work

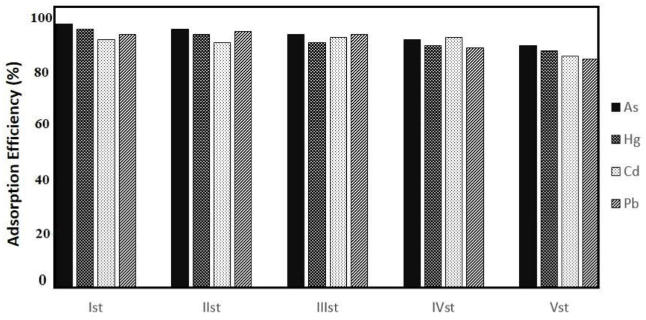

Fig. 13. Sorbent recycled runs against elimination efficiency of As^{3+}, Hg^{2+}, Cd^{2+}, and Pb^{2+} ions.

was repetitive for five times. The regenerated sorbent was used again for five sorption cycles by the 30 mg L^{-1} toxic ions solution in the analogous situation as described. The consequences illustrated that the outcomes of the recycled sorbent for eliminating cations were approximately the same as those for the new ones even after recycling five times (Fig. 13). Abatement of sorption capacity in repetitive cycles may be due to the translocation of some adsorbed fictionalizer molecules from the exfoliated bentonite surface. Meanwhile, the entire translocation of MPTMS did not happen as substantial sorption efficiency detected in the next cycles. The appropriate sorption capacity of this sorbent in the following sorption cycles made it a respectable option for multi-cyclic use. In addition, the achieved information of ICP studies revealed that only less than 9% of MEAB is leached after five running cycles.

4. Conclusions

In the present research, we presented a facile method for the synthesis of thiol (–SH) functional groups onto an exfoliated bentonite clay for the first time. The thiol group treated exfoliated bentonite was very capable and effective in eliminating individual toxic ions such as As(III), Pb(II), Hg(II), and Cd(II) from an aqueous solution. The study of the sorption features showed that different factors such as interaction time, pH, primary ions concentration, sorbent dosage, and turbulence played key parts in the sorption performance. The highest sorption revenue was acquired at pH = 8, the sorption ratio was established comparatively quickly, and the equilibrium was acquired within 30 min. In optimum conditions, thiol treated exfoliated bentonite was distinguished as an effective sorbent with the highest uptake effectiveness.

Acknowledgment

The financial support of this study by Tarbiat Modares University (Tehran, Iran) is gratefully acknowledged.

References

[1] L. Lin, X. Xu, C. Papelis, P. Xu, Innovative use of drinking water treatment solids for heavy metals removal from desalination concentrate: synergistic effect of salts and natural organic matter, Chem. Eng. Res. Des., 120 (2017) 231–239.

[2] S.K. Yadanaparthi, D. Graybill, R.V. Wandruszka, Adsorbents for the removal of arsenic, cadmium, and lead from contaminated waters, J. Hazard. Mater., 171 (2009) 1–15.

[3] M. Saeedi, M. Hosseinzadeh, M. Rajabzadeh, Competitive heavy metals adsorption on natural bed sediments of Jajrood River, Iran, Environ. Earth Sci., 62 (2011) 519–527.

[4] H. Hamad, Z. Ezzeddine, F. Lakisa, H. Rammal, M. Srour, A. Hijazi, An insight into the removal of Cu (II) and Pb (II) by aminopropyl-modified mesoporous carbon CMK-3: adsorption capacity and mechanism, Mater. Chem. Phys., 178 (2016) 57–64.

[5] M. Hua, S. Zhang, B. Pan, W. Zhang, L. Lv, Q. Zhang, Heavy metal removal from water/wastewater by nanosized metal oxides: a review, J. Hazard. Mater., 211–212 (2012) 317–331.

[6] S.A. Sajjadi, A. Mohammadzadeh, H.N. Tran, G.L. Dotto, Z.R. Lopičić, S. Sivamani, A. Rahmani-Sani, A. Ivanets, A.H. Bandegharaei, Efficient mercury removal from wastewater by pistachio wood wastes-derived activated carbon prepared by chemical activation using a novel activating agent, J. Environ. Manage., 223 (2018) 1001–1009.

[7] D. Mohan, C.U. Pittman Jr, Arsenic removal from water/wastewater using adsorbents—a critical review, J. Hazard. Mater., 142 (2007) 1–53.

[8] P. Li, X.-q. Zhang, Y.J. Chen, T.Y. Bai, H.Z. Lian, X. Hu, One-pot synthesis of thiol- and amine-bifunctionalized mesoporous silica and applications in uptake and speciation of arsenic, RSC Adv., 4 (2014) 49421–49428.

[9] A. Chen, X. Xin, J. Xu, Y. Bian, Removal of aqueous arsenic using abundant boehmite coated zeolite, Desal. Wat. Treat., 77 (2017) 342–348.

[10] E.K. Guechi, D. Beggas, Removal of cadmium (II) from water using fibre fruit lufa as biosorbent, Desal. Wat. Treat., 94 (2017) 181–188.

[11] A. Ivanets, V. Srivastava, N.V. Kitikova, I. Shashkova, M. Sillanpää, Non-apatite Ca-Mg phosphate sorbent for removal of toxic metal ions from aqueous solutions, J. Environ. Chem. Eng., 5 (2017) 2010–2017.

[12] V.V. Tomina, N.V. Stolyarchuk, I.V. Melnyk, Y. Zub, T.F. Kouznetsova, V.G. Prozorovich, A.I. Ivanets, Composite sorbents based on porous ceramic substrate and hybrid amino- and mercapto-silica materials for Ni(II) and Pb(II) ions removal, Sep. Purif. Methods, 175 (2017) 391–398.

[13] F.E. Soetaredjo, Y.H. Ju, S. Ismadji, A. Ayucitra, Removal of Cu(II) and Pb(II) from wastewater using biochar-clay nanocomposite, Desal. Wat. Treat., 82 (2017) 188–200.

[14] A.I. Ivanets, V.G. Prozorovich, T.F. Kouznetsova, A.V. Radkevich, A.M. Zarub, Mesoporous manganese oxides prepared by sol-gel method: synthesis, characterization and sorption properties towards strontium ions, J. Environ. Nano Monit. Manage., 6 (2016) 261–269.

[15] V.J. Inglezakis, M.D. Loizidou, H.P. Grigoropoulou, Ion exchange of Pb^{2+}, Cu^{2+}, Fe^{3+}, and Cr^{3+} on natural clinoptilolite: selectivity determination and influence of acidity on metal uptake, J. Colloid Interface Sci., 261 (2003) 49–54.

[16] S. Muhammad, M.T. Shah, S. Khan, Health risk assessment of heavy metals and their source apportionment in drinking water of Kohistan region, northern Pakistan, Microchem. J., 98 (2011) 334–343.

[17] A. Ates, E. Altintig, H. Demirel, M. Yilmaz, Comparative study on adsorptive removal of Cu, Pb, Zn heavy metals by modified perlite composites, Desal. Wat. Treat., 98 (2017) 244–253.

[18] A.I. Ivanets, V. Srivastava, M.Y. Roshchina, M. Sillanpää, V.G. Prozorovich, V.V. Pankovd, Magnesium ferrite nanoparticles as a magnetic sorbent for the removal of Mn^{2+}, Co^{2+}, Ni^{2+} and Cu^{2+} from aqueous solution, Ceram. Int., 44 (2018) 9097–9104.

[19] J.H. Huang, G.M. Zeng, C.F. Zhou, X. Li, S.B. He, Adsorption of surfactant micelles and Cd^{2+}/Zn^{2+} in micellar-enhanced ultrafiltration, J. Hazard. Mater., 183 (2010) 287–293.

[20] X. Ying, Z. Fang, Experimental research on heavy metal wastewater treatment with dipropyl dithiophosphate, J. Hazard. Mater., 137 (2006) 1636–1642.

[21] M.A. Tofighy, T. Mohammadi, Copper ions removal from aqueous solutions using acid-chitosan functionalized carbon nanotubes sheets, Desal. Wat. Treat., 57 (2016) 15384–15396.

[22] A.I. Ivanetsa, A.I. Rat'ko, T.A. Azarova, S.M. Azarov, S.H. Al-Khowaiter, O. Al-Harbi, V. Shemchonok, V.A. Dobysh, V.A. Tarasevich, V.E. Agabekov, A.A. Rat'ko, Preparation and properties of microfiltration membranes based on natural crystalline SiO_2, Ceram. Int., 40 (2014) 12343–12351.

[23] A. Da'browski, Z. Hubicki, P. Podkościelny, E. Robens, Selective removal of the heavy metal ions from waters and industrial wastewaters by ion-exchange method, Chemosphere, 56 (2004) 91–106.

[24] J. Qian, M. Qiu, Z. Zeng, W. Xue, Study on ion-exchange behavior of Cu^{2+} and Ni^{2+} with a high-efficiency resin, Desal. Wat. Treat., 93 (2017) 152–162.

[25] L. Perelomov, B. Sarkar, M.M. Rahman, A. Goryacheva, R. Naidu, Uptake of lead by Na-exchanged and Al-pillared bentonite in the presence of organic acids with different functional groups, Appl. Clay Sci., 119 (2016) 417–423.

[26] Z. Lou, W. Zhang, X. Hu, H. Zhang, Synthesis of a novel functional group-bridged magnetized bentonite adsorbent: characterization, kinetics, isotherm, thermodynamics and regeneration, Chin. J. Chem. Eng., 25 (2017) 587–594.

[27] A. Shahzad, W. Miran, K. Rasool, M. Nawaz, J. Jang, S.R. Lim, D.S. Lee, Heavy metals removal by EDTA-functionalized chitosan graphene oxide nanocomposites, RSC Adv., 7 (2017) 9764–9771.

[28] A. Naghizadeh, M. Kamranifar, A.R. Yari, M.J. Mohammadi, Equilibrium and kinetics study of reactive dyes removal from aqueous solutions by bentonite nanoparticles, Desal. Wat. Treat., 97 (2017) 329–337.

[29] L. Zhu, R. Zhu, Simultaneous sorption of organic compounds and phosphate to inorganic–organic bentonites from water, Sep. Purif. Technol., 54 (2007) 71–76.

[30] J. Ma, J. Qi, C. Yao, B. Cui, T. Zhang, D. Li, A novel bentonite-based adsorbent for anionic pollutant removal from water, Chem. Eng. J., 200–202 (2012) 97–100.

[31] R. Zhu, Q. Chen, Q. Zhou, Y. Xi, J. Zhu, H. He, Adsorbents based on montmorillonite for contaminant removal from water: a review, Appl. Clay Sci., 123 (2016) 239–258.

[32] W. Mo, Q. He, X. Su, S. Ma, J. Feng, Z. He, Preparation and characterization of a granular bentonite composite adsorbent and its application for Pb^{2+} adsorption, Appl. Clay Sci., 159 (2018) 68–73.

[33] D. Aggarwal, M. Goyal, R.C. Bansal, Adsorption of chromium by activated carbon from aqueous solution, Carbon, 37 (1999) 1989–1997.

[34] H. Yanagisawa, Y. Matsumoto, M. Machida, Adsorption of Zn(II) and Cd(II) ions onto magnesium and activated carbon composite in aqueous solution, Appl. Surf. Sci., 256 (2010) 1619–1623.

[35] P. Stathi, K. Litin, D. Gournis, T.S. Giannopoulos, Y. Deligiannakis, Physicochemical study of novel organoclays as heavy metal ion adsorbents for environmental remediation, J. Colloid Interface Sci., 316 (2007) 298–309.

[36] T. de Mattos Amadio, D. Hotza, Bentonites functionalized by impregnation with TiO_2, Ag, Pd and Au nanoparticles, Appl. Clay Sci., 146 (2017) 1–6.

[37] M.G.A. Vieira, A.F. Almeida Neto, M.L. Gimenes, M.G.C. da Silva, Removal of nickel on Bofe bentonite calcined clay in porous bed, J. Hazard. Mater., 176 (2010) 109–118.

[38] D. Wan, W. Li, G. Wang, K. Chen, L. Lu, Q. Hu, Adsorption and heterogeneous degradation of rhodamine B on the surface of magnetic bentonite material, Appl. Surf. Sci., 349 (2015) 988–996.

[39] S.P. Patil, B. Bethi, G.H. Sonawane, V.S. Shrivastava, S. Sonawane, Efficient adsorption and photocatalytic degradation of Rhodamine B dye over Bi_2O_3-bentonite nanocomposites: a kinetic study, J. Ind. Eng. Chem., 34 (2016) 356–363.

[40] J. Ma, D. Huang, W. Zhang, J. Zou, Y. Kong, J. Zhu, S. Komarneni, Nanocomposite of exfoliated bentonite/g-C_3N_4/Ag_3PO_4 for enhanced visible-light photocatalytic decomposition of Rhodamine B, Chemosphere, 162 (2016) 269–276.

[41] Z. Xia, L. Baird, N. Zimmerman, M. Yeager, Heavy metal ion removal by thiol functionalized aluminum oxide hydroxide nanowhiskers, Appl. Surf. Sci., 416 (2017) 565–573.

[42] A. Walcarius, M. Etinnę C. Delacote, Uptake of inorganic Hg (II) by organically modified silicates: aqueous: influence of pH and choride concentration on the binding pathways and electrochemical monitoring of the processes, Anal. Chim. Acta., 508 (2004) 87–98.

[43] W. Gan, L. Gao, X. Zhan, J. Li, Preparation of thiol-functionalized magnetic sawdust composites as an adsorbent to remove heavy metal ions, RSC Adv., 6 (2016) 37600–37609.

[44] A.M.F. Guimarães, V.S.T. Ciminelli, W.L. Vasconcelos, Smectite organofunctionalized with thiol groups for adsorption of heavy metal ions, Appl. Clay Sci., 42 (2009) 410–414.

[45] L. Mercier, C. Detellier, Preparation, characterization, and applications as heavy metals sorbents of covalently grafted thiol functionalities on the interlamellar surface of montmorillonite, Environ. Sci. Technol., 29 (1995) 318–1323.

[46] M. Rezapour, H. Abdollahi, H. Khorrami, J.T. Valmazuei, Application of raw, HCl- and H_2SO_4-activated bentonite as adsorbents for the removal of Zn^{2+} and Pb^{2+} from aqueous solution, Desal. Wat. Treat., 57 (2016) 3654–3663.

[47] H. Mabrouki, D.E. Akretche, Diclofenac potassium removal from water by adsorption on natural and pillared clay, Desal. Wat. Treat., 57 (2016) 6072–6080.

[48] Z. Huang, Y. Li, W. Chen, J. Shi, Modified bentonite adsorption of organic pollutants of dye wastewater, Mater. Chem. Phys., 202 (2017) 266–276.

[49] D.M. Manohar, B.F. Noeline, T.S. Anirudhan, Adsorption performance of Al-pillared bentonite clay for the removal of cobalt(II) from aqueous phase, Appl. Clay Sci., 31 (2006) 194–206.

[50] C. Zhang, J. Sui, J. Li, Y. Tang, W. Cai, Efficient removal of heavy metal ions by thiol-functionalized superparamagnetic carbon nanotubes, Chem. Eng. J., 210 (2012) 45–52.

[51] N.N. Ab Kadir, M. Shahadat, S. Ismail, Formulation study for softening of hard water using surfactant modified bentonite adsorbent coating, Appl. Clay Sci., 137 (2017) 168–175.

[52] A. Walcarius, M. Etienne, J. Bessiere, Rate of access to the binding sites in organically modified silicates. Amorphous silica gels grafted with amine or thiol groups, Chem. Mater., 14 (2002) 2757–2766.

[53] W.M. Gitari, T. Ngulube, V. Masindi, J.R. Gumbo, Defluoridation of groundwater using Fe^{3+}-modified bentonite clay: optimization of adsorption conditions, Desal. Wat. Treat., 53 (2015) 1578–1590.

[54] C.Y. Cao, L.K. Meng, Y.H. Zhao, Adsorption of phenol from wastewater by organo-bentonite, Desal. Wat. Treat., 52 (2014) 3504–3509.

[55] J. Wang, H. Ma, W. Yuan, W. He, S. Wang, J. You, Synthesis and characterization of an inorganic/organic-modified bentonite and its application in methyl orange water treatment, Desal. Wat. Treat., 52 (2014) 7660–7672.

[56] Y. Angar, N.E. Djelali, S. Kebbouche-Gana, Kinetic and thermodynamic studies of the ammonium ions adsorption onto natural Algerian bentonite, Desal. Wat. Treat., 57 (2016) 25696–25704.

[57] A. Afkhami, M.S. Tehrani, H. Bagheri, Simultaneous removal of heavy-metal ions in wastewater samples using nano-alumina modified with 2,4-dinitrophenylhydrazine, J. Hazard. Mater., 181 (2010) 836–844.

[58] E. Boyacı, A. Çağır, T. Shahwan, A.E. Erŏglu, Synthesis, characterization and application of a novel mercapto- and amine-bifunctionalized silica for speciation/sorption of inorganic arsenic prior to inductively coupled plasma mass spectrometric determination, Talanta, 85 (2011) 1517–1525.

[59] R. Hasanzadeh, P.N. Moghadam, N. Bahri-Laleh, M. Sillanpää, Effective removal of toxic metal ions from aqueous solutions: 2-Bifunctional magnetic nanocomposite base on novel reactive PGMA-MAn copolymer@Fe_3O_4 nanoparticles, J. Colloid Interface Sci., 490 (2017) 727–746.